Supporting Information

Metal Acetylacetonates as a Source of Metals for Aqueous Synthesis of Metal-Organic Frameworks

Ceren Avci-Camur, [†]Javier Perez-Carvajal,[†] Inhar Imaz,* [†] and Daniel Maspoch* [† ‡]

[†]Catalan Institute of Nanoscience and Nanotechnology (ICN2), CSIC and The Barcelona Institute of Science and Technology, Campus UAB, Bellaterra, 08193 Barcelona, Spain

[‡] Institució Catalana de Recerca i Estudis Avançats (ICREA), 08100 Barcelona, Spain

E-mail: inhar.imaz@icn2.cat; daniel.maspoch@icn2.cat

The following electronic supporting information contains 20 pages, 5 tables, and 23 figures

Section 1. UiO-66-NH_2

Table S1: Summary of the yield and S_{BET} values obtained for different samples in the optimisation of acetic acid concentration for the synthesis of UiO-66-NH_2 (V_{tot}: 6 mL; reagent concentration: 0.4 M).

Acetic acid (v/v)	Yield (%)	S_{BET} (m^2 g^{-1})
8%	-	-
17%	55	772
25%	60	1008
33%	65	1069
50%	70	1106
66%	60	1064

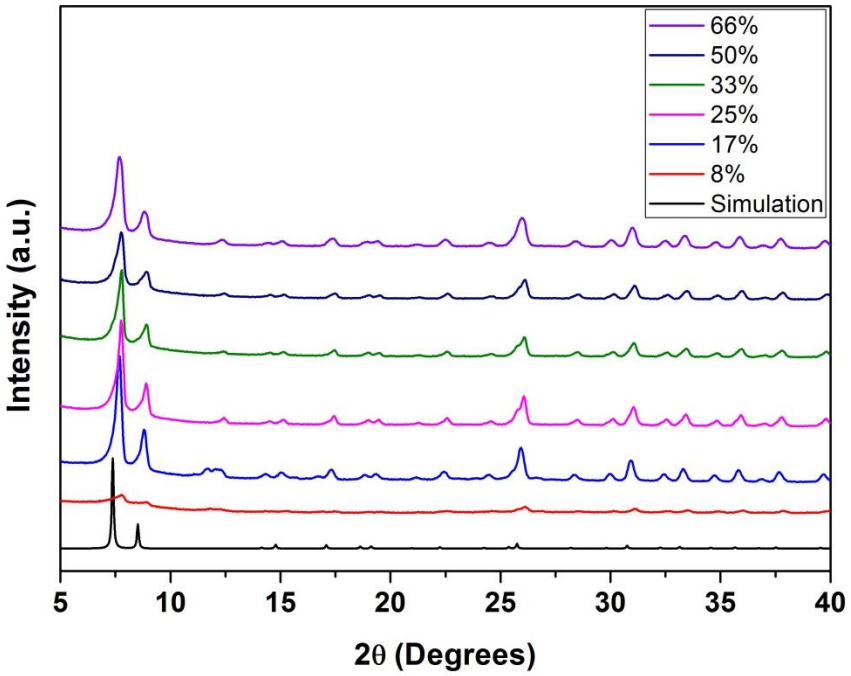

Figure S1: XRPD patterns for the UiO-66-NH_2 samples synthesised by using different concentrations of acetic acid in water (v/v).

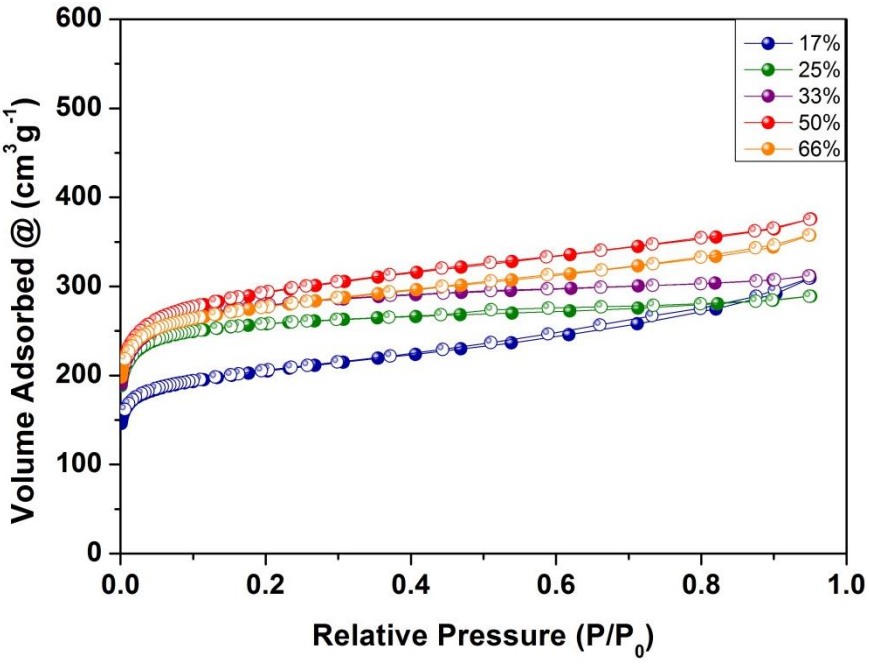

Figure S2: N_2 adsorption (filled dots) and desorption (empty dots) isotherms at 77 K for UiO-66-NH_2 samples synthesised by using different concentrations of acetic acid in water (v/v).

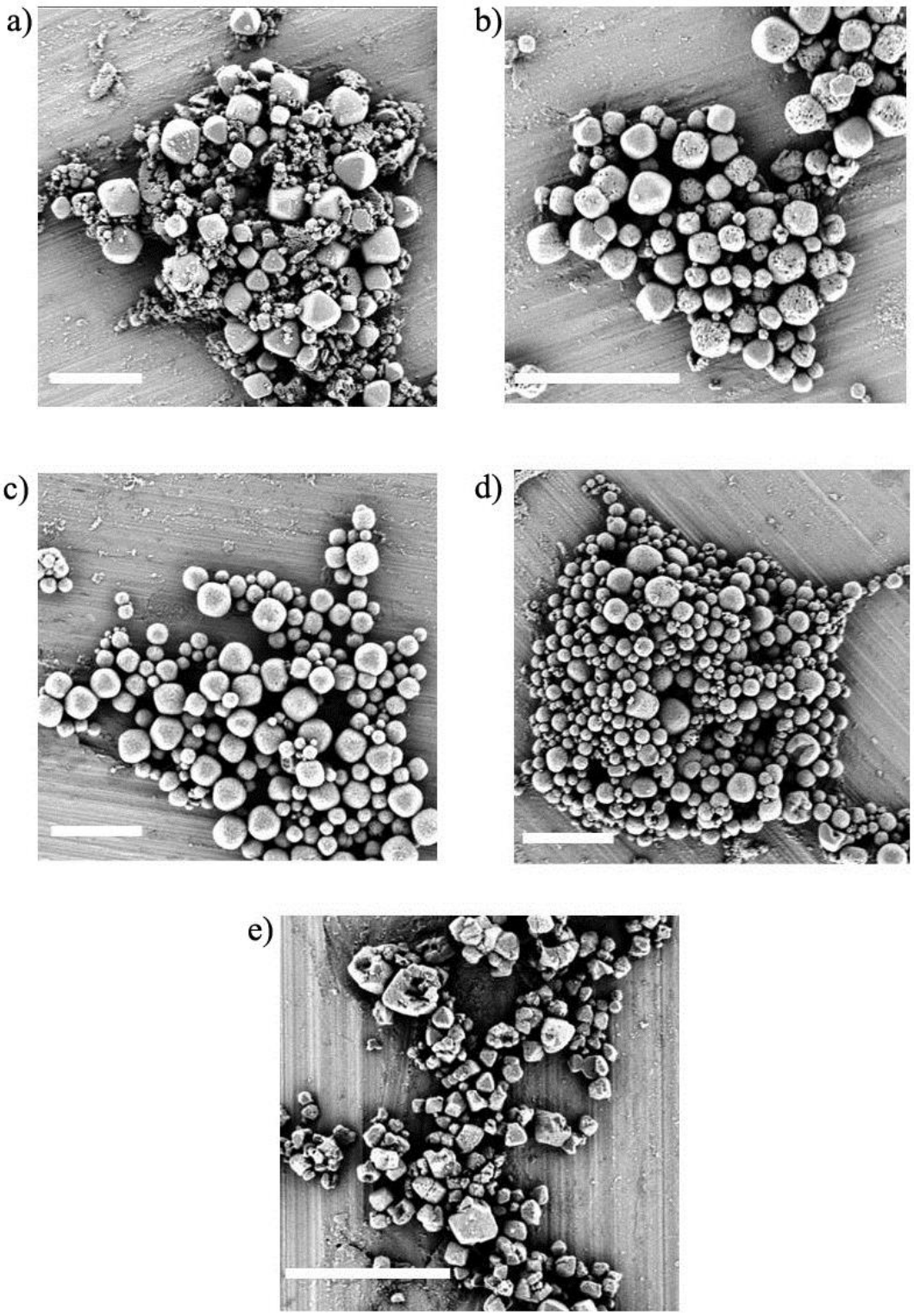

Figure S3: FESEM images of the UiO-66-NH_2 samples synthesised by using different concentrations of acetic acid in water (v/v): 17% (a), 25% (b), 33% (c), 50% (d) and 66% (e). Scale bars: 3 µm.

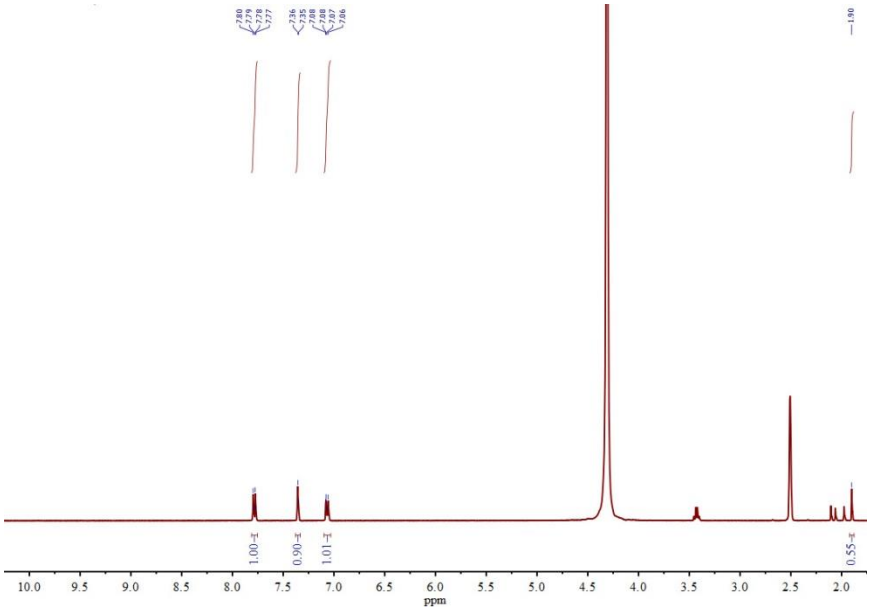

Figure S4: NMR spectrum of the digested UiO-66-NH_2 (synthesized by using 50 % acetic acid) in HF/$DMSO_{-d6}$.

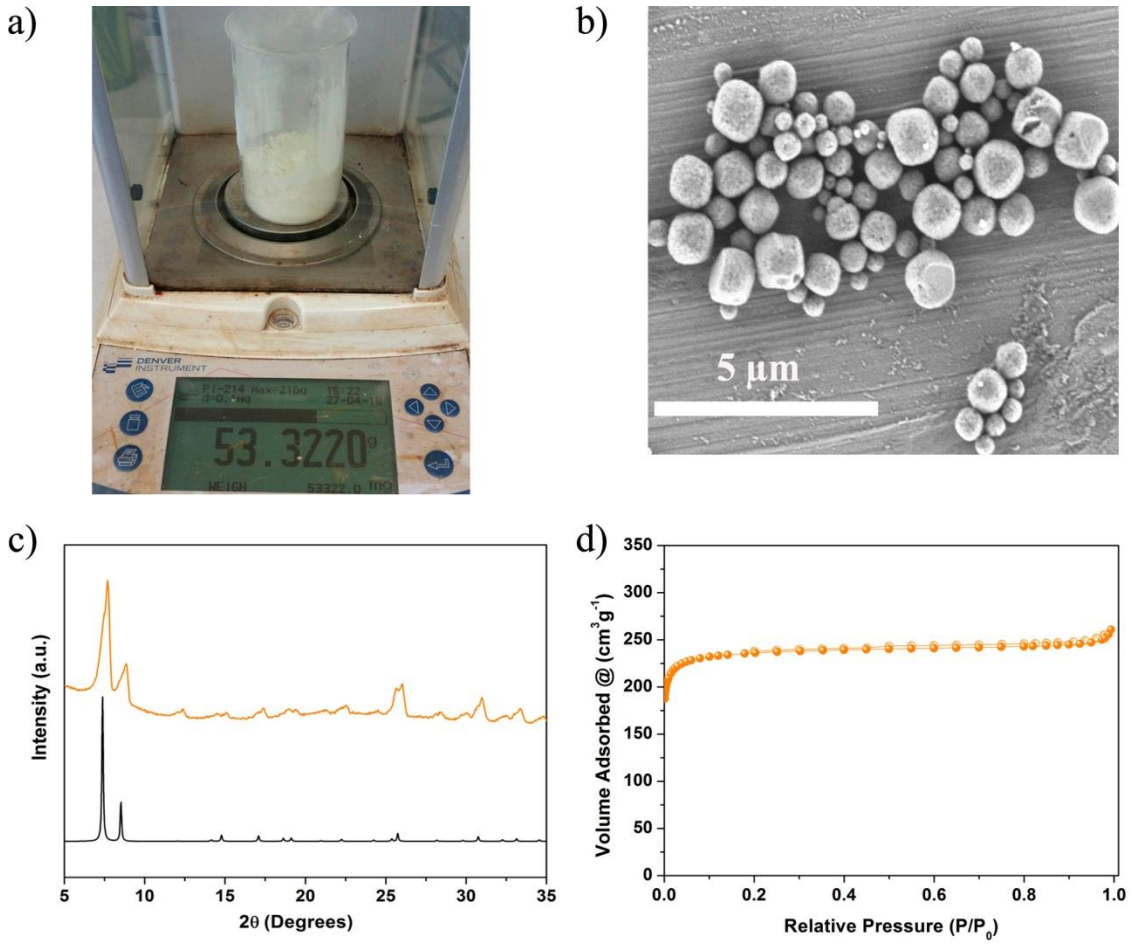

Figure S5: Photograph (a), FESEM image (b), XRPD patterns of simulated (black) and synthesized UiO-66-NH_2 (orange) (c) and N_2 adsorption (filled dots) and desorption (empty dots) isotherms at 77 K of the UiO-66-NH_2 (53 g) powder.

Section 2. Zr-fumarate

Table S2: Summary of the yield and S_{BET} values obtained for different samples in the optimisation of acetic acid concentration for the synthesis of Zr-fumarate (V_{tot}: 6 mL; reagent concentration: 0.4 M).

Acetic acid (v/v)	Yield (%)	S_{BET} (m^2 g^{-1})
8%	-	-
17%	70	750
25%	88	797
33%	88	1249
50%	83	1220
66%	87	917

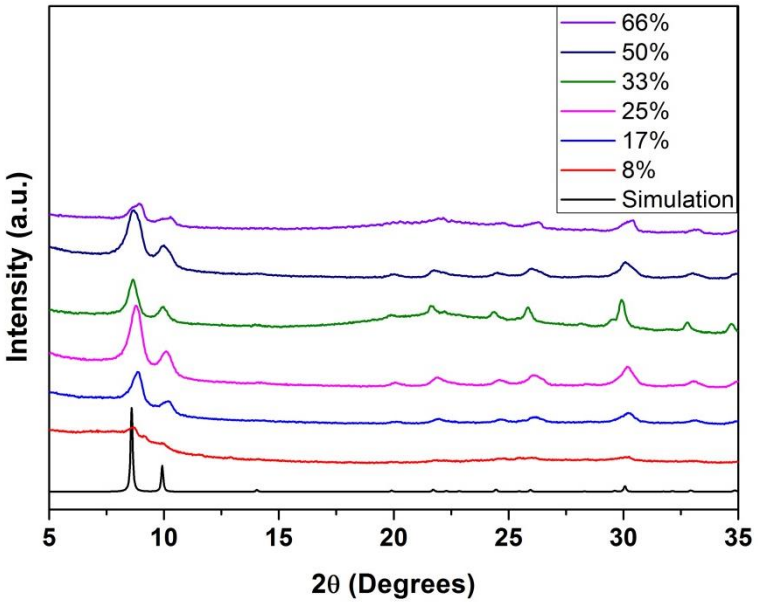

Figure S6: XRPD patterns for the Zr-fumarate samples synthesised by using different concentrations of acetic acid in water (v/v).

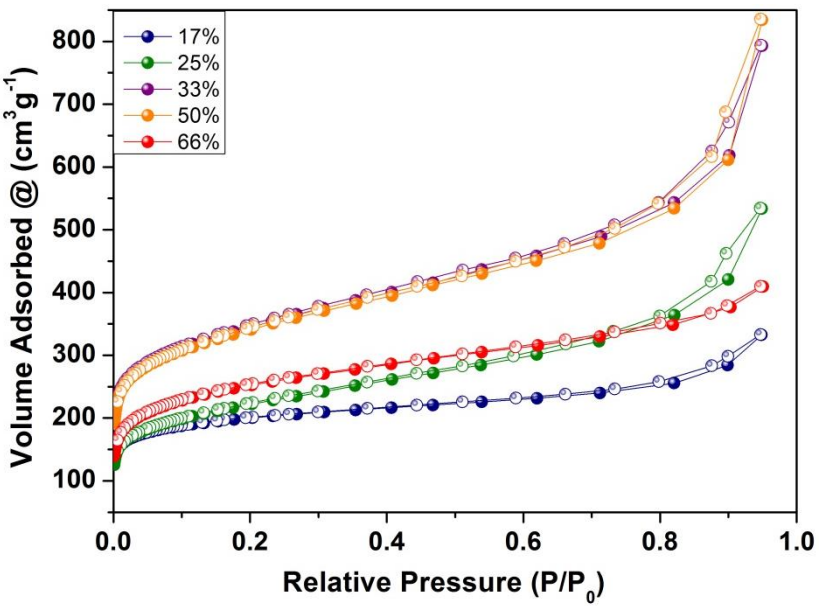

Figure S7: N_2 adsorption (filled dots) and desorption (empty dots) isotherms at 77 K for Zr-fumarate samples synthesised by using different concentrations of acetic acid in water (v/v).

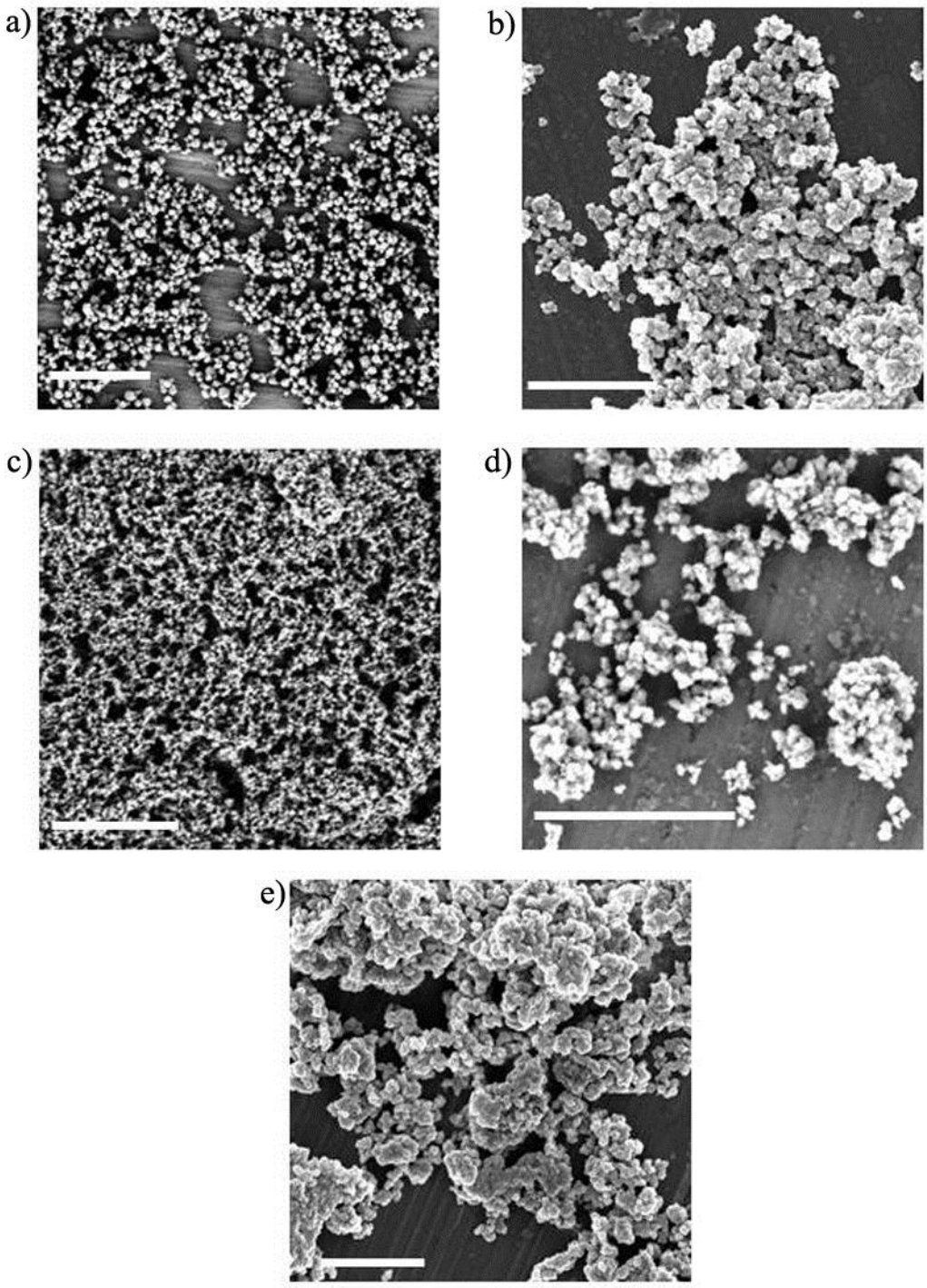

Figure S8: FESEM images of the Zr-fumarate samples synthesised by using different concentrations of acetic acid in water (v/v): 17% (a), 25% (b), 33% (c), 50% (d) and 66% (e) Scale bars: 1 µm.

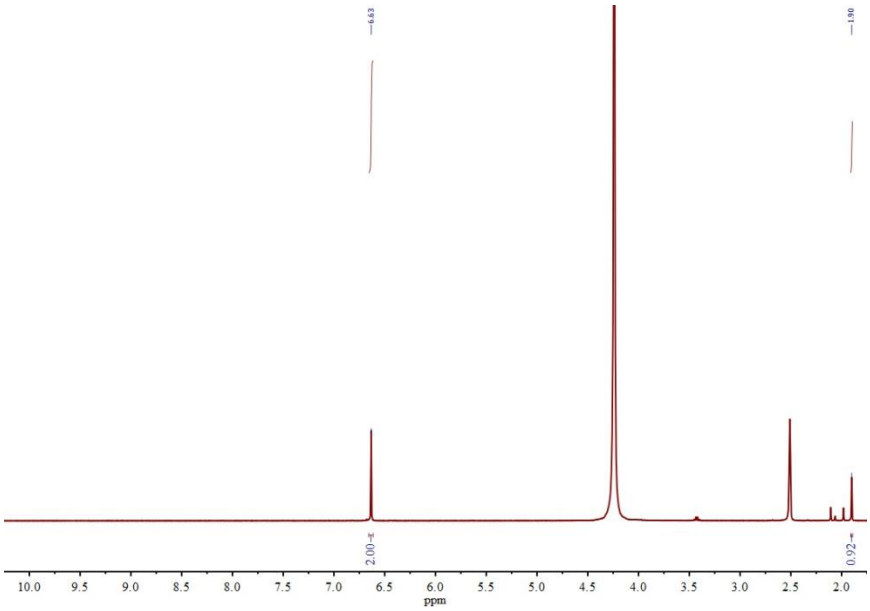

Figure S9: NMR spectrum of the digested Zr-fumarate (synthesized by using 30 % acetic acid) in HF/$DMSO_{-d6}$.

Section 3. UiO-66-$(OH)_2$

Table S3: Summary of the yield and S_{BET} values obtained for different samples in the optimisation of acetic acid concentration in the synthesis of UiO-66-$(OH)_2$ (V_{tot}: 6 ml, reagent concentration: 0.4 M).

Acetic Acid (v/v)	Yield (%)	S_{BET} (m^2 g^{-1})
8%	-	-
17%	-	-
25%	90	200
33%	93	200
50%	94	330
66%	94	733

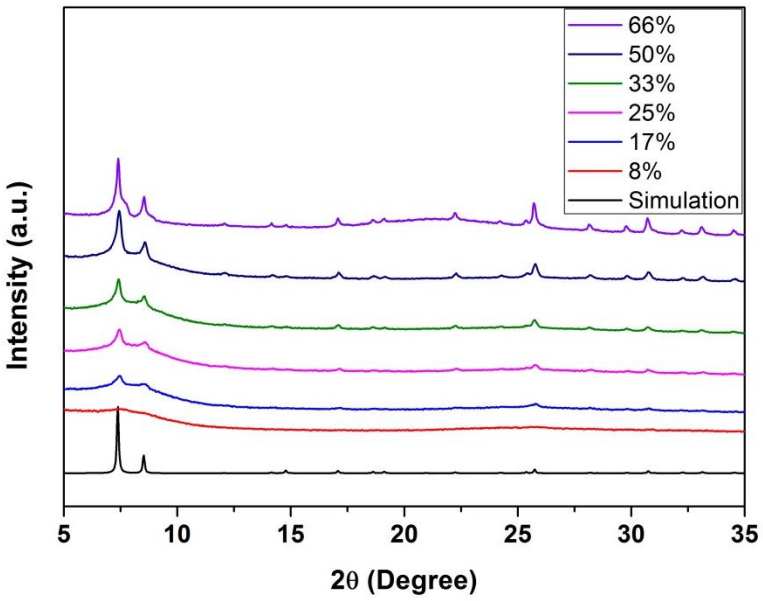

Figure S10: XRPD patterns of the UiO-66-$(OH)_2$ samples synthesised by using different concentrations of acetic acid in water (v/v).

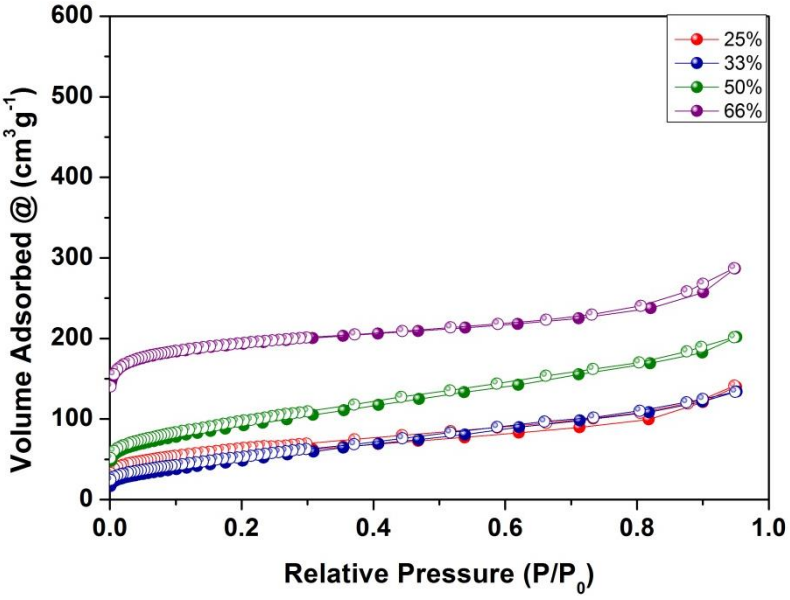

Figure S11: N_2 adsorption (filled dots) and desorption (empty dots) isotherms at 77 K for UiO-66-$(OH)_2$ samples synthesised by using different concentrations of acetic acid in water (v/v).

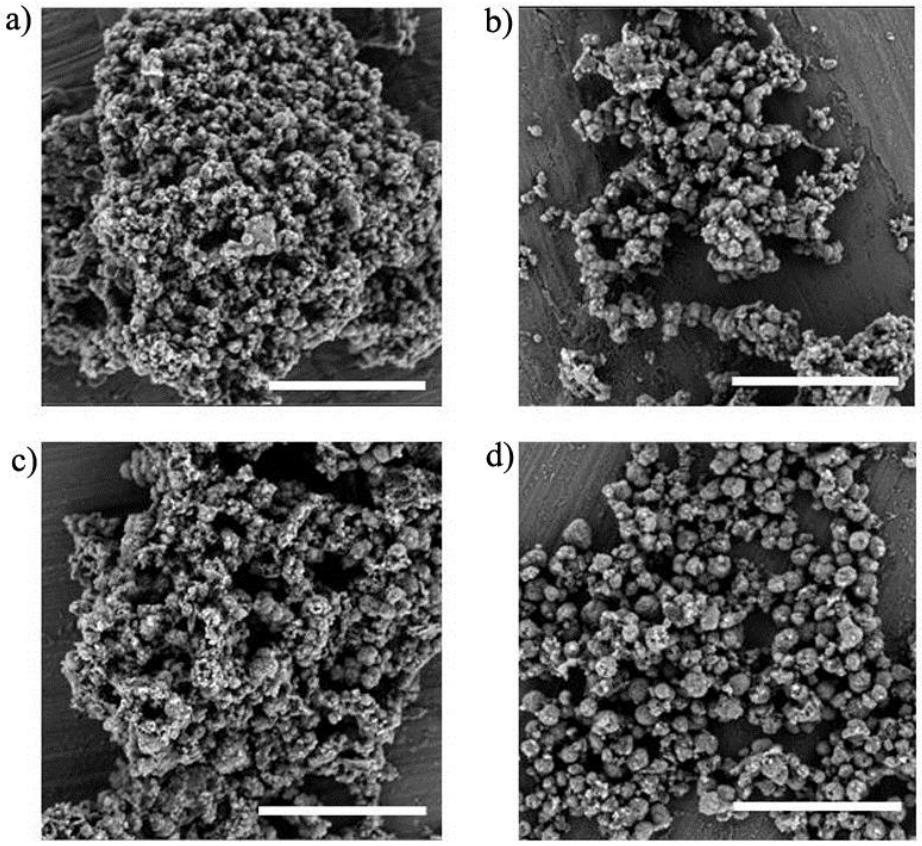

Figure S12: FESEM images of the UiO-66-$(OH)_2$ samples synthesised by using different concentrations of acetic acid in water (v/v): 25% (a), 33% (b), 50% (c) and 66% (d). Scale bars: 3 μm.

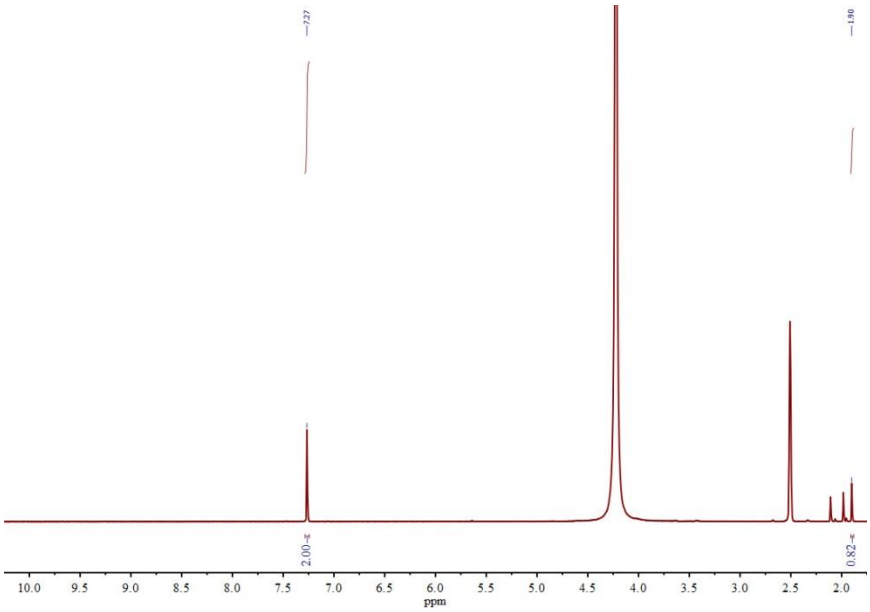

Figure S13: NMR spectrum of the digested UiO-66-$(OH)_2$ (synthesized by using 66 % acetic acid) in HF/$DMSO_{-d6}$.

Section 4. UiO-66-$(COOH)_2$

Table S4: Summary of the yield and S_{BET} values obtained for different samples in the optimisation of acetic acid concentration for the synthesis of UiO-66-$(COOH)_2$ (V_{tot}: 6 mL; reagent concentration: 0.75 M).

Acetic acid (v/v)	Yield (%)	S_{BET} (m^2 g^{-1})
17%	88	415
33%	90	538
50%	89	518
66%	91	542

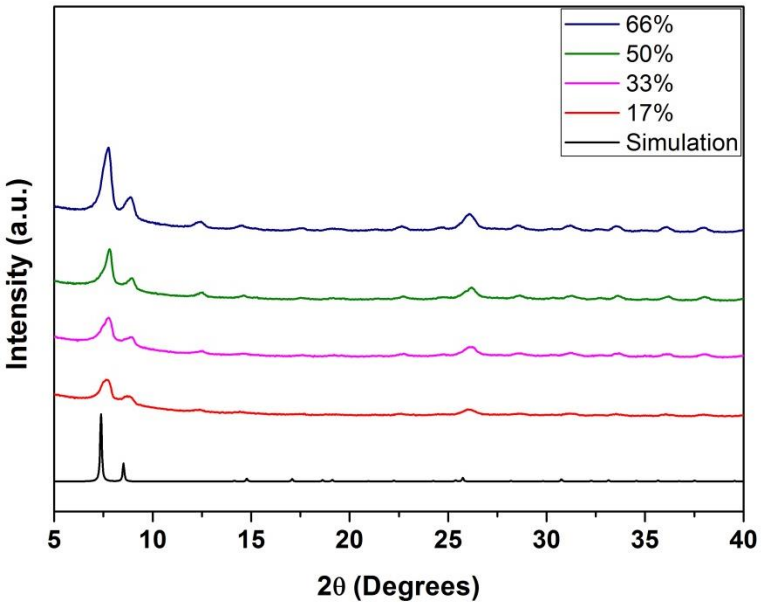

Figure S14: XRPD patterns for the UiO-66-$(COOH)_2$ samples synthesised by using different concentrations of acetic acid in water (v/v).

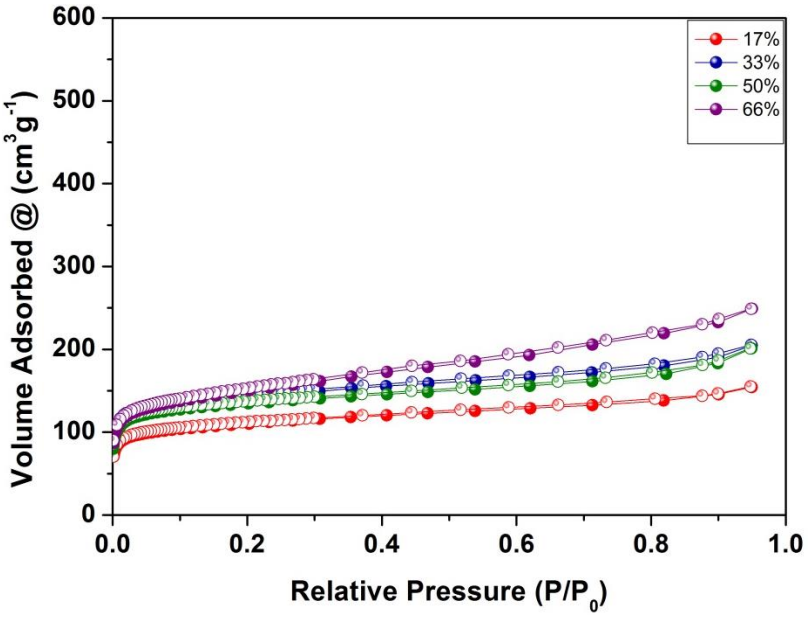

Figure S15: N_2 adsorption (filled dots) and desorption (empty dots) isotherms at 77 K for the UiO-66-$(COOH)_2$ samples synthesised by using different concentrations of acetic acid in water (v/v).

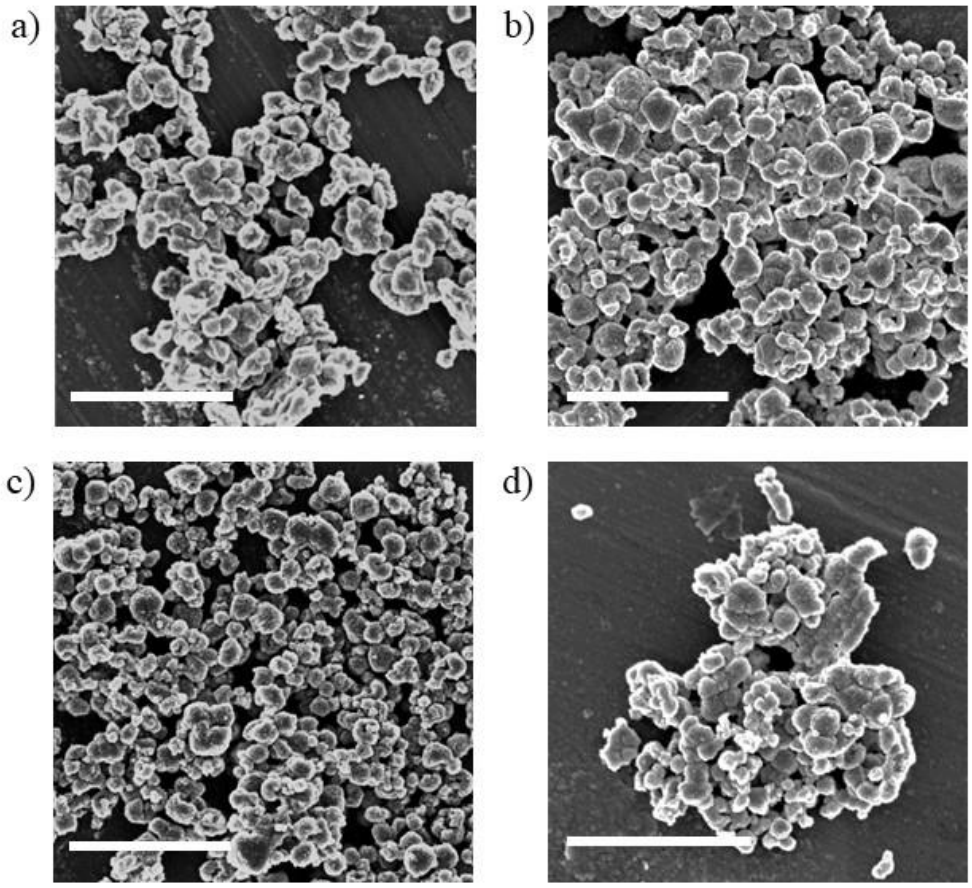

Figure S16: FESEM images of the UiO-66-$(COOH)_2$ samples synthesised by using different concentrations of acetic acid in water (v/v): 17% (a), 33% (b), 50% (c) and 66% (d). Scale bars: 2 µm.

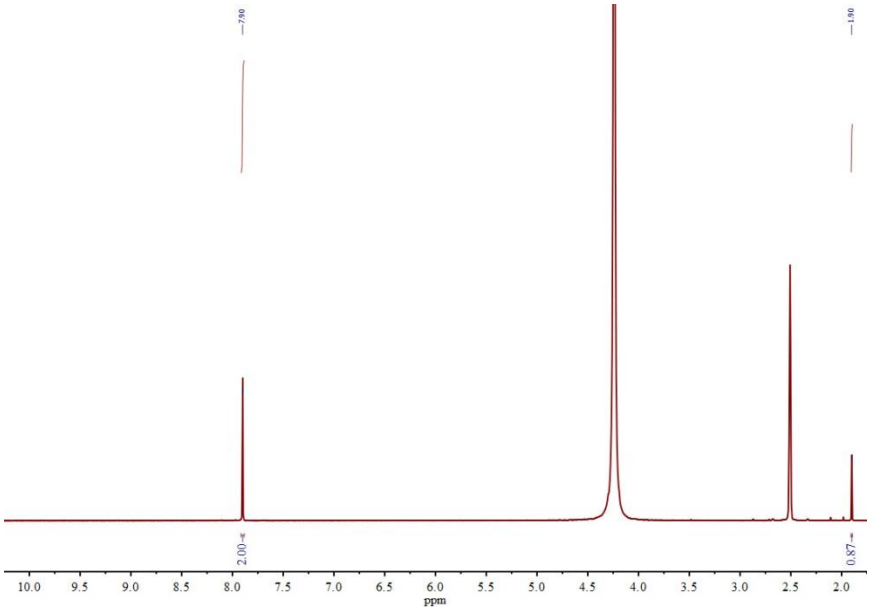

Figure S17: NMR spectrum of the digested UiO-66-$(COOH)_2$ (synthesized by using 33 % acetic acid) in HF/DMSO-d6.

Section 5. UiO-66-COOH

Table S5: Summary of the yield and S_{BET} values obtained for different samples in the optimisation of acetic acid concentration for the synthesis of UiO-66-COOH (V_{tot}: 6 mL; reagent concentration: 0.75 M).

Acetic acid (v/v)	Yield (%)	S_{BET} (m^2 g^{-1})
17%	-	-
33%	88	268
50%	91	452
66%	90	538

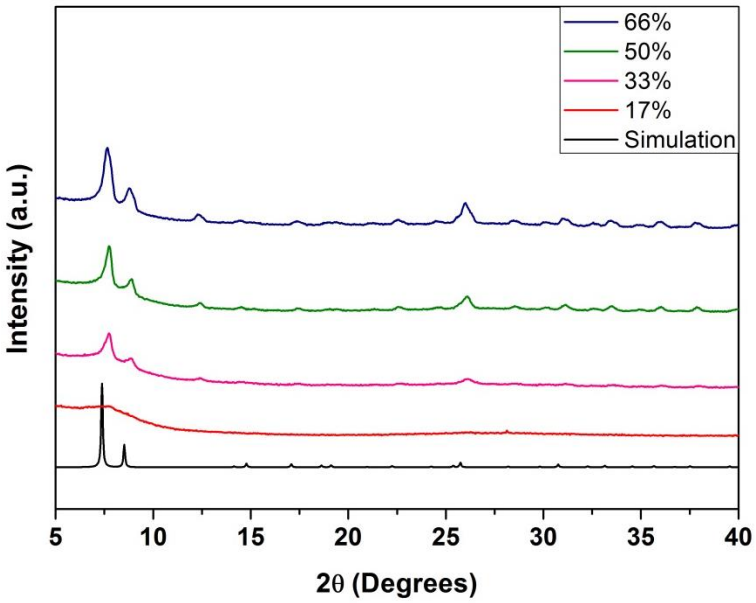

Figure S18: XRPD patterns for the UiO-66-COOH samples synthesised by using different concentrations of acetic acid in water (v/v).

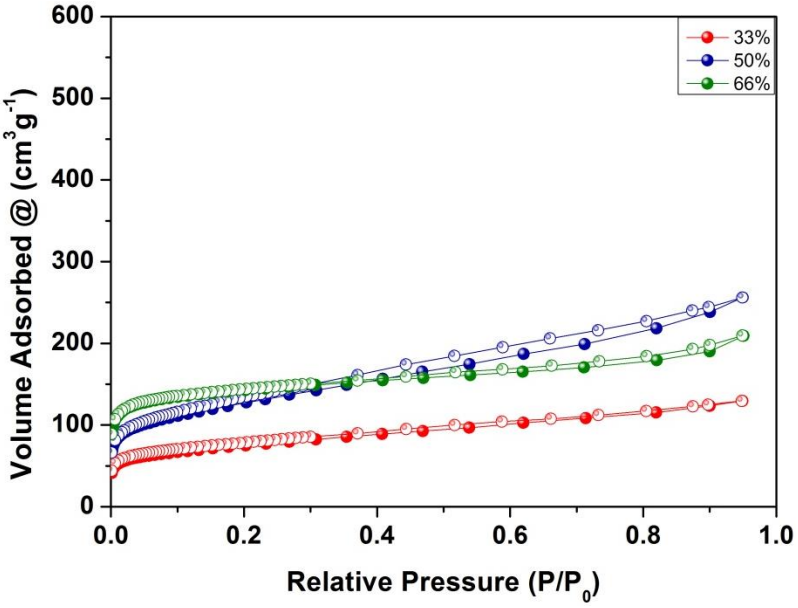

Figure S19: N_2 adsorption (filled dots) and desorption (empty dots) isotherms at 77 K for the UiO-66-COOH samples synthesised by using different concentrations of acetic acid in water (v/v).

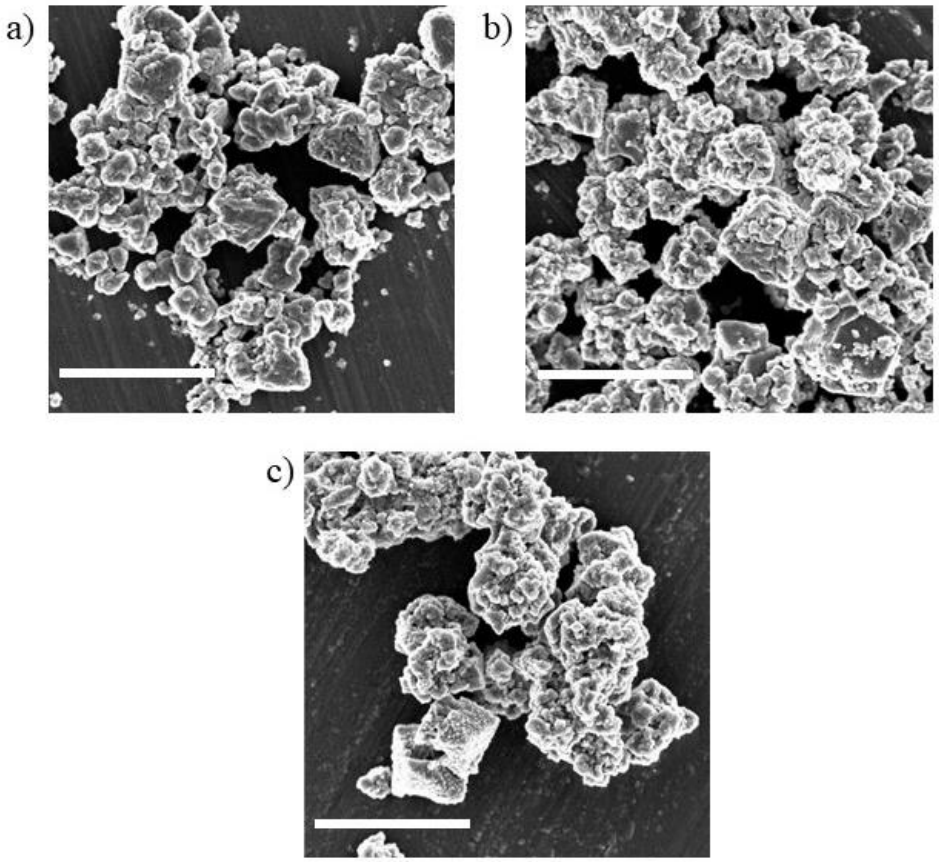

Figure S20: FESEM images of the UiO-66-COOH samples synthesised by using different concentrations of acetic acid in water (v/v): 33% (a), 50% (b) and 66% (c). Scale bars: 2 µm.

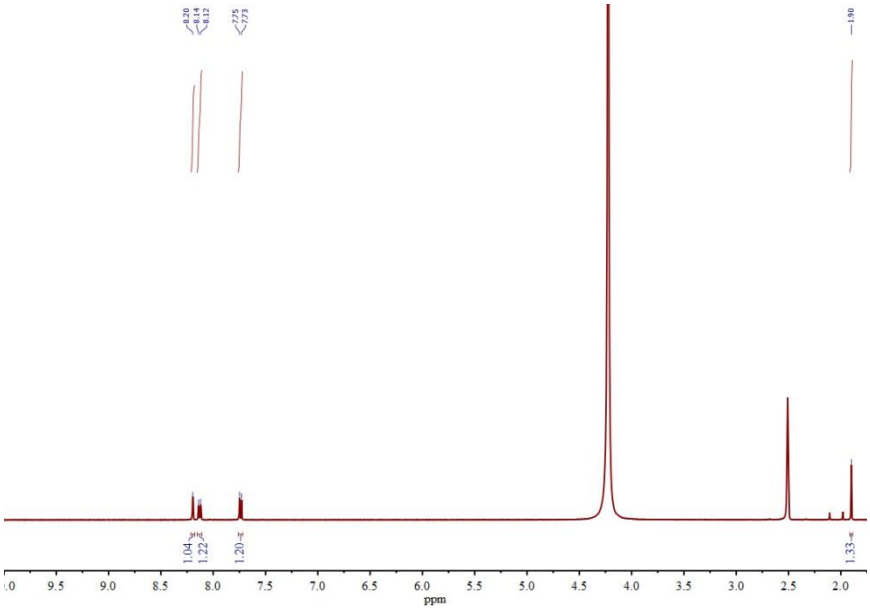

Figure S21: NMR spectrum of the digested UiO-66-COOH (synthesized by using 66 % acetic acid) in HF/DMSO$_{-d6}$.

Section 6. MIL-88A and CAU-10

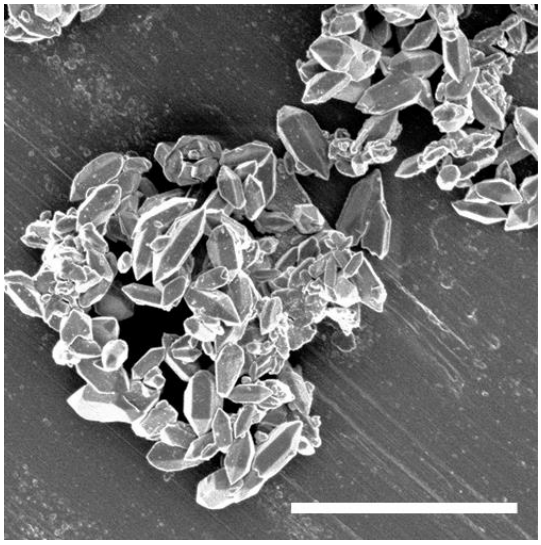

Figure S22: Representative FESEM image of the hexagonal rod-like crystals of MIL-88A. Scale bar: 3 µm.

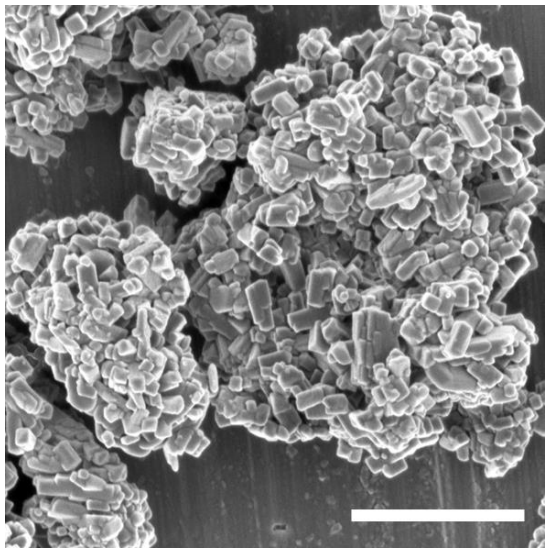

Figure S23: Representative FESEM image of the submicrometre crystals of CAU-10. Scale bar: 1 µm.